Passively mode locked femtosecond $Tm:Sc_2O_3$ laser at 2.1 μm

A. A. Lagatsky[1,*], P. Koopmann[2,3], P. Fuhrberg[3], G. Huber[2], C. T. A. Brown[1], and W. Sibbett[1]

[1]*SUPA, School of Physics and Astronomy, University of St Andrews, North Haugh, St Andrews, KY16 9SS, UK*

[2]*Institute of Laser-Physics, University of Hamburg, Luruper Chaussee 149, D-22761 Hamburg, Germany*

[3]*LISA Laser Products, Max-Planck-Strasse 1, D-27191 Katlenburg-Lindau, Germany*

**Corresponding author: aal2@st-andrews.ac.uk*

Received November 4, 2011; accepted December 12, 2011;
posted December 14, 2011 (Doc. ID 157737); published February 1, 2012

We report on the passive mode locking of a $Tm^{3+}:Sc_2O_3$ laser at 2.1 μm using a semiconductor saturable absorber mirror based on InGaAsSb quantum wells. Transform-limited 218 fs pulses are generated with an average power of 210 mW. A maximum output power of 325 mW is produced during mode locking with the corresponding pulse duration of 246 fs at a pulse repetition frequency of 124.3 MHz. A Ti:sapphire laser is used as the pump source operating at 796 nm. © 2012 Optical Society of America

OCIS codes: 140.4050, 140.7090, 140.5680, 140.3070, 140.3580, 160.3380.

Ultrashort-pulse lasers that operate in the 2 μm spectral region and produce relatively high average powers (100s of milliwatts and above) are of particular interest for the development of broadband coherent sources such as optical parametric oscillators or supercontinua in the mid-IR (~2–10 μm) spectral region. Such optical frequency comb systems can be utilized for real-time, high-sensitivity and high-resolution detection of absorption features of molecular species present in the so-called "molecular fingerprint" region [1,2]. Representative applications include those in environmental monitoring [3], industrial process control, detection of drugs and explosive materials, as well as human breath analysis [4]. Other potential implementations of 2 μm ultrafast lasers relate to free-space optical communications [5], imaging techniques in turbid media such as optical coherence tomography [6], and the three-dimensional microstructuring of semiconductors [7].

So far, only a few lasers capable of producing nanojoule-energy femtosecond pulses around 2 μm have been demonstrated [8,9]. These include a Tm-doped fiber laser that was passively mode locked using an additive-pulse mode-locking technique to produce pulses with energies of up to 4 nJ (167 mW of average power) that were compressed externally to a duration of 173 fs. However, this involved a rather complex configuration that required a combination of fiber and free-space optics as well as an external-cavity pulse compressor.

Recently, we have demonstrated the efficient generation of femtosecond pulses directly from Tm-doped and Tm,Ho codoped solid-state crystalline lasers by using a semiconductor saturable absorber mirror (SESAM) for passive mode locking [10–12]. In particular, 191 fs pulses were produced from Tm, Ho:$NaY(WO_4)_2$ around 2060 nm and a Tm:$KY(WO_4)_2$ laser generated 386 fs pulses with an average power of 235 mW at 2029 nm. Regarding further development of diode-pumped, high-power, 2 μm solid-state femtosecond lasers, Tm-doped crystals having characteristic broadband and relatively homogeneous gain spectra (preferably extending beyond 2 μm) and accompanying good thermomechanical properties represent excellent candidate gain media. In this respect, the recently investigated Tm-doped sesquioxide crystals (Lu_2O_3 and Sc_2O_3) that possess high thermal conductivities and demonstrate efficient and high-power cw operation in the range ~1930–2150 nm are especially interesting [13,14]. It should be noted that long wavelength generation (>2 μm) from a Tm-laser is advantageous for stable passive mode locking because the presence of strong water vapor absorption bands in the ~1800–2000 nm region can prevent broadband mode locking and give rise to Q-switching instabilities. Previously, only passive mode locking of a Tm:Lu_2O_3 laser has been reported. This system incorporated a carbon nanotube saturable absorber to produce 31 ps pulses at 1965 nm [15].

Here we report, for the first time to our knowledge, the passive mode locking of a Tm-doped Sc_2O_3 laser by utilizing a quantum-well-based SESAM. Transform-limited 218 fs pulses were produced at a center wavelength of 2107 nm with an average power exceeding 210 mW.

The 1.5 at.% doped $Tm:Sc_2O_3$ crystal was grown by the heat-exchanger method, which allows the production of high-quality rare-earth-ion-doped sesquioxides [16]. The $Tm:Sc_2O_3$ can be efficiently pumped at a local absorption peak at 796 nm, and its emission spectrum extends beyond 2100 nm due to the strong ground-state Stark-level splitting of ~990 cm^{-1}. Depending on the inversion population level, the maximum gain peaks are located at around 1990 nm or 2120 nm, and both bands are appropriate for ultrashort pulse generation (Fig. 1). Further spectroscopic data for the Tm-doped Sc_2O_3 can be found in [14,17].

The experimental assessments were carried out with a Ti:sapphire pump laser that produced up to 2.6 W at 796 nm. An asymmetric, astigmatically compensated Z-fold resonator was configured with two high-reflectivity ($R > 99.2\%$ from 1770 to 2100 nm) folding (full angle of 18°) mirrors M_1 and M_2 having radii of curvature of 100 mm, an output coupler (OC) with 1.2%, 2.3%, or 4% of transmission at 2.1 μm and a SESAM (Fig. 2). The resonator was designed to operate in the middle of stability zone II to ensure a second mode waist on the saturable absorber element. The SESAM used for passive mode locking initiation and stabilization is based on an ion-implanted InGaAsSb quantum-well structure and

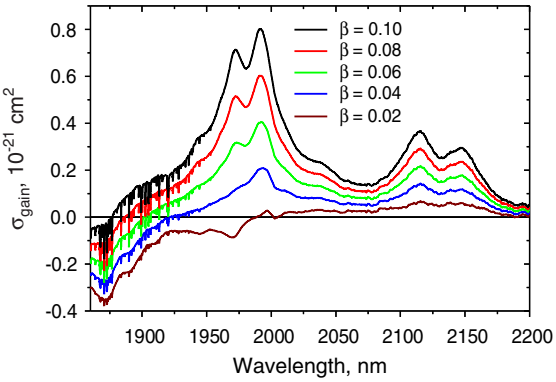

Fig. 1. (Color online) Inversion-dependent gain cross sections of $Tm:Sc_2O_3$. $\sigma_{gain}(\lambda) = \beta\sigma_e - (1-\beta)\sigma_a$, where σ_e and σ_a are emission and absorption cross sections, respectively.

characterized by an initial reflection of 99.5%–98.1% in the 2–2.1 μm range [11]. It was mounted on a copper heat sink to ensure efficient heat removal during prolonged laser operation. An 8 mm long Brewster-cut $Tm:Sc_2O_3$ crystal was placed between two curved folding mirrors where the minimum laser beam mode radius was calculated to be 36 μm. A p-polarized pump beam was focused into the gain medium via an 80 mm focal length lens and mirror M_1 ($T > 99\%$ at 976 nm) to a spot radius of 31.5 μm ($1/e^2$ intensity) measured in air at the location of the input facet of the crystal.

During cw operation (a high-reflectivity plane mirror was used instead of the SESAM and without the prism pair), the $Tm:Sc_2O_3$ laser produced a maximum output power of 660 mW at 1998 nm when the 4% OC was used. With an output coupling of 1.2%, laser operation was observed at 2115 nm (300 mW of output power) and dual-wavelength operation (1998 and 2115 nm) took place at 2.3% of output coupling. With the SESAM in place, lasing was realized at around 2 μm only, and although mode locking was observed, the pulses were relatively long (~800 fs) and the laser exhibited rather unstable behavior with Q-switching instabilities and occasional spectral jumps between 2 and 2.1 μm. To stabilize the $Tm:Sc_2O_3$ laser operation at around 2.1 μm only, which is more favorable for ultrashort pulse generation due to broader gain features and negligible water vapor absorption, a short-wave pass filter (SWPF) was introduced into the cavity. It had transmission of more than 20% around 2000 nm and broadband high reflectivity ($R > 99.9\%$) that started from 2050 nm. With this arrangement, the $Tm:Sc_2O_3$ laser operated at around 2115 nm only, and it produced maximum power of up to 605 and 535 mW with the 4% and 2.3% OCs, respectively, in cw operation.

When the mode radius of the intracavity beam on the SESAM was set to be 190 μm and the 2.3% OC was used, stable mode-locked operation was observed at a center wavelength of 2111 nm, and maximum average output power of 325 mW was produced. The pulse repetition frequency was measured using a fast InGaAs photodiode and a radio-frequency spectrum analyzer and was detected to be 124.3 MHz. Stable single-pulse mode locking with no evidence of Q-switching instabilities was observed in a range of output powers from 105 to 325 mW, whereas Q-switched mode locking became evident at lower intracavity powers, noticeably, when the fluence on the SESAM was below 32.4 μJ/cm^2 (Fig. 3). The pulse durations, which were derived from the intensity autocorrelation traces, assuming sech^2 pulse intensity profiles, varied from 730 fs at the mode-locking threshold to 246 fs [Figs. 3 and 4(a)] at the maximum output power as a soliton mode-locking model would predict [18]. The corresponding optical spectra broadened from 6.7 to 19.6 nm [Fig. 4(b)] (FWHM) with center wavelengths that varied only slightly from 2111 to 2113 nm. The time-bandwidth products ranged from 0.31 to 0.33.

When the output coupling was changed to 1.2%, shorter pulse durations of 218 fs were obtained [Fig. 4(c)] with a maximum average power of 210 mW. The corresponding optical spectrum was centered at 2107 nm with a bandwidth of 21.7 nm, implying a time–bandwidth product of 0.32 [Fig. 4(d)]. Kelly sidebands [19] were observed on both sides of the spectrum. During these experimental arrangements, the cavity mode spot size on the SESAM was adjusted to be 220 μm in radius and the repetition frequency of the pulses was measured to be 118.8 MHz.

A pair of IR-grade fused silica prisms with tip-to-tip separation of 8.5 cm was used during mode locking for control of the intracavity net group delay dispersion (GDD). Each prism was placed at a minimum deviation and caused only about 5% of average output power reduction.

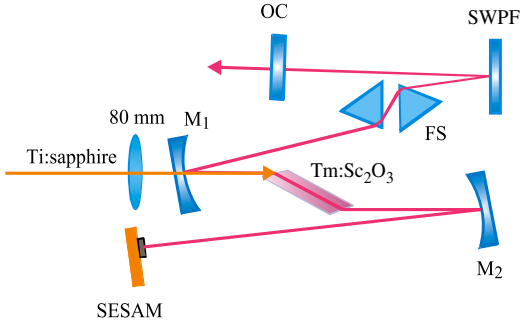

Fig. 2. (Color online) Schematic of the mode-locked $Tm:Sc_2O_3$ laser. M_1 and M_2, plano–concave high-reflector mirrors, $r_1 = r_2 = -100$ mm; OC, output coupler; SWPF, short-wave pass filter; FS, pair of IR-grade fused silica prisms.

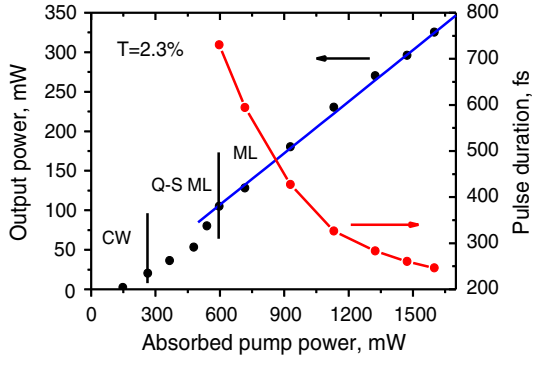

Fig. 3. (Color online) Input–output average power characteristics and the pulse duration as a function of absorbed pump power for the $Tm:Sc_2O_3$ laser. CW, continuous-wave operation; Q-S ML, Q-switched mode locking; ML, cw mode locking.

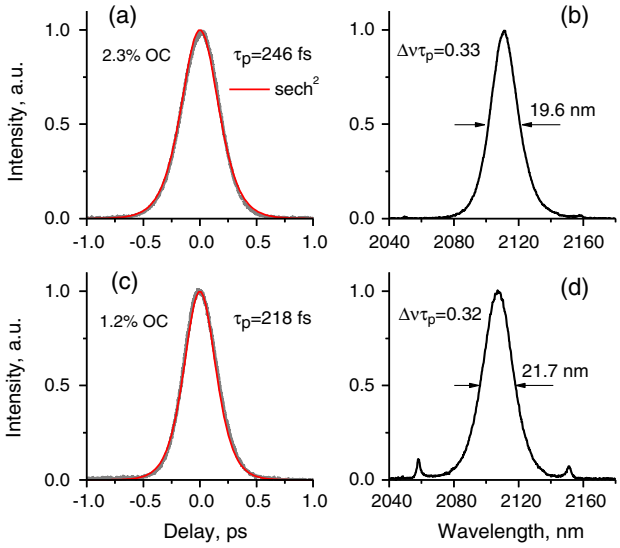

Fig. 4. (Color online) Intensity autocorrelation traces and the corresponding optical spectra of the mode-locked Tm:Sc_2O_3 laser for output couplings of 2.3% [(a), (b)] and 1.2% [(c), (d)].

The total round-trip GDD during mode locking at 2.1 μm was estimated to be -2573 fs^2, resulting from 1096 fs^2 in the Tm:Sc_2O_3 crystal (68.5 fs^2/mm), -984 fs^2 due to material dispersion of fused silica (-123 fs^2/mm), and -2685 fs^2 due to the angular dispersion in the prism pair.

In conclusion, passive mode locking of the Tm-doped Sc_2O_3 laser near 2.1 μm is reported for the first time to the authors' knowledge. By deploying an ion-implanted InGaAsSb quantum-well-based SESAM and a prism-pair dispersion management approach, transform-limited pulses as short as 218 fs were produced at 2107 nm with an average power of 210 mW. The maximum achieved average power from this femtosecond laser was 325 mW at a pulse repetition frequency of 124.3 MHz that implied a generated pulse energy of 2.6 nJ. We believe that further power scaling toward the multiwatt level is feasible from a mode-locked Tm:Sc_2O_3 laser with direct diode pumping [14]. Additionally, when the gain bandwidth of Tm:Sc_2O_3 around 2.1 μm is taken into account, it is expected that further reduction of the pulse duration will be achieved when the SESAM parameters are further optimized.

The funding support of the UK Engineering and Physical Sciences Research Council is gratefully acknowledged.

References

1. E. Sorokin, I. T. Sorokina, J. Mandon, G. Guelachvili, and N. Picqué, Opt. Express **15**, 16540 (2007).
2. F. Adler, P. Maslowski, A. Foltynowicz, K. C. Cossel, T. C. Briles, I. Hartl, and J. Ye, Opt. Express **18**, 21861 (2010).
3. W. C. Swann and N. R. Newbury, Opt. Lett. **31**, 826 (2006).
4. M. J. Thorpe, D. Balslev-Clausen, M. S. Kirchner, and J. Ye, Opt. Express **16**, 2387 (2008).
5. V. W. S. Chan, IEEE J. Sel. Top. Quantum Electron. **6**, 959 (2000).
6. B. E. Bouma, L. E. Nelson, G. J. Tearney, D. J. Jones, M. E. Brezinski, and J. G. Fujimoto, J. Biomed. Opt. **3**, 76 (1998).
7. R. R. Gattass and E. Mazur, Nat. Photon. **2**, 219 (2008).
8. M. Engelbrecht, F. Haxsen, A. Ruehl, D. Wandt, and D. Kracht, Opt. Lett. **33**, 690 (2008).
9. F. Haxsen, D. Wandt, U. Morgner, J. Neumann, and D. Kracht, Opt. Express **18**, 18981 (2010).
10. A. A. Lagatsky, F. Fusari, S. Calvez, S. V. Kurilchik, V. E. Kisel, N. V. Kuleshov, M. D. Dawson, C. T. A. Brown, and W. Sibbett, Opt. Lett. **35**, 172 (2010).
11. A. A. Lagatsky, X. Han, M. D. Serrano, C. Cascales, C. Zaldo, S. Calvez, M. D. Dawson, J. A. Gupta, C. T. A. Brown, and W. Sibbett, Opt. Lett. **35**, 3027 (2010).
12. A. A. Lagatsky, S. Calvez, J. A. Gupta, V. E. Kisel, N. V. Kuleshov, C. T. A. Brown, M. D. Dawson, and W. Sibbett, Opt. Express **19**, 9995 (2011).
13. P. Koopmann, S. Lamrini, K. Scholle, P. Fuhrberg, K. Petermann, and G. Huber, Opt. Lett. **36**, 948 (2011).
14. P. Koopmann, S. Lamrini, K. Scholle, P. Fuhrberg, K. Petermann, and G. Huber, in *Advanced Solid-State Photonics*, Technical Digest (Optical Society of America, 2011), paper ATuA5.
15. A. Schmidt, U. Griebner, V. Petrov, S. Y. Choi, W. B. Cho, D.-I. Yeom, F. Rotermund, P. Koopmann, K. Petermann, G. Huber, and P. Fuhrberg, in *Europhoton Conference* (European Physical Society, 2010), paper TuC3.
16. R. Peters, C. Kränkel, K. Petermann, and G. Huber, J. Cryst. Growth **310**, 1934 (2008).
17. L. Fornasiero, N. Berner, B.-M. Dicks, E. Mix, V. Peters, K. Petermann, and G. Huber, in *Advanced Solid State Lasers*, Vol. **26** of OSA Trends in Optics and Photonics, M. M. Fejer, H. Injeyan, and U. Keller, eds. (Optical Society of America, 1999), p. 450.
18. F. X. Kartner, I. D. Jung, and U. Keller, IEEE J. Sel. Top. Quantum Electron. **2**, 540 (1996).
19. S. M. J. Kelly, Electron. Lett. **28**, 806 (1992).